Activities and Findings:

1. **Glider Simulator**

Model of Glider

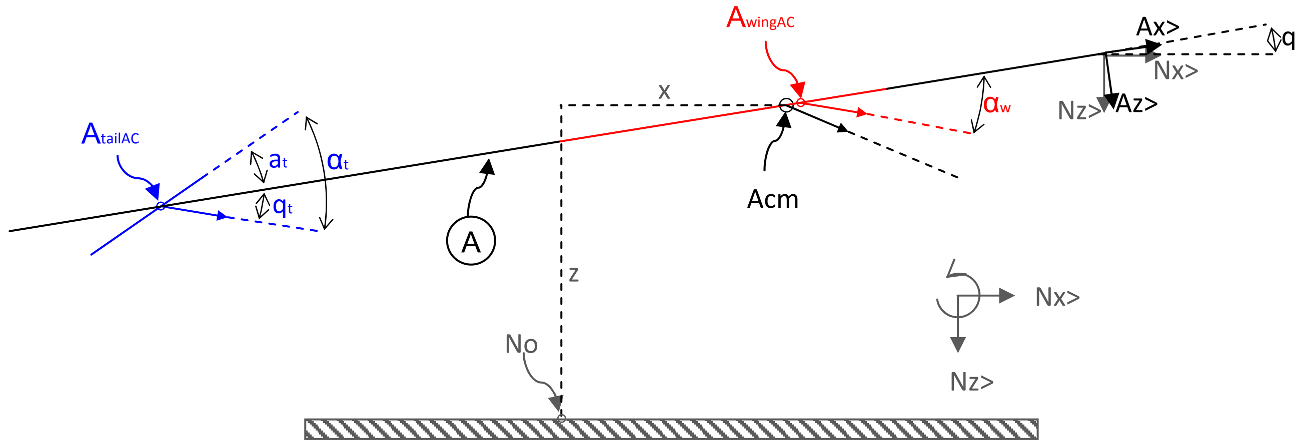

Simplified model of a glider:

To simplify the analysis of a glider, the pitch dynamics was studied assuming that the yaw and roll dynamics are passively stable. Hence, only the 2D dynamics in the Nx Nz plane was considered.

To simulate a launch, the of the glider can be initialized with a take-off speed, take-off angle and take-off angular velocity.

Assumptions:

1. Yaw and roll dynamics are passively stable
2. Wing and tail are modeled as flat plates

Table of identifiers

Quantity	**Identifier**	**Type**	**(Initial) Value(s)**
air density	rho	Constant	1.2041 kg/m^3
local gravitational constant	g	Constant	9.80665 m/sec^2
mass of glider	m	Constant	0.4kg
A's moment of inertia about Acm for Ay>	Iayy	Constant	223.6 g*mm^2
B's moment of inertia about Bcm for By>	s_w	Constant	73.1 g*mm^2
C's moment of inertia about Acm for Cy>	s_t	Constant	350 g*mm^2
ax> measure of distance from A_cm to A_tail_ac	dt	Constant	54.4 g*mm^2
ax> measure of distance from A_cm to A_wing_ac	dw		
q is defined as the angle between Nx> and Ax> in the positive Ay> direction	q	dependent variable	
	q'		
Nx> measure of Acm from No	x	dependent variable	(0 m)
	x'		
Nz> measure of Bo from No	z	dependent variable	(-1.5m)
	z'		
Work of forces on the system	N_W_A	dependent variable	(0 joules)
Control Input from tail: angle between tail and Ax>	a_t	specified	

Physics

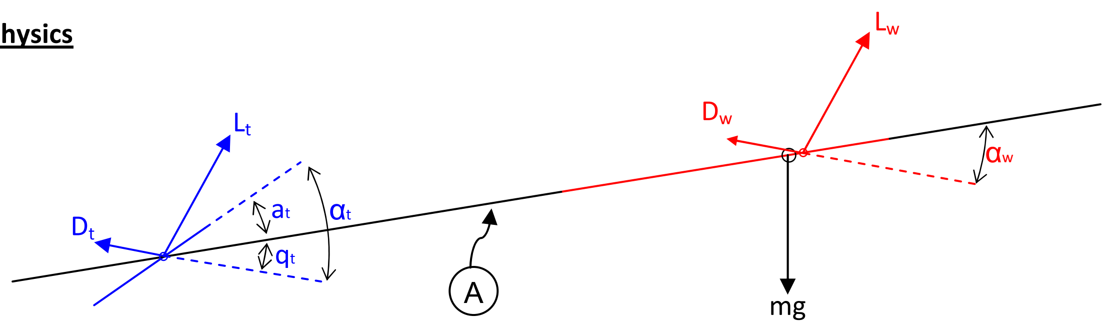

$\alpha_t = q_t + a_t$

The forces acting on the glider are lift and drag at A_{wingAC} and A_{tailAC} and weight at A_{cm}.

Due to the flat plate assumption of the wing and tail, the lift and drag coefficients are modeled as:

$C_L = 2\sin(\alpha)\cos(\alpha)$

$C_D = 2\sin^2(\alpha)$

The equations of motion are derived from Newton/Euler

$\vec{F}^A = m.{}^N\vec{a}^{Acm}$

$\vec{D}_t + \vec{L}_t + \vec{D}_w + \vec{L}_w = m{}^N\vec{a}^{Acm}$

$\vec{D}_t + \vec{L}_t + \vec{D}_w + \vec{L}_w = m(\ddot{x}\vec{n}_x + \ddot{z}\vec{n}_z)$ - (1)

Where lift and drag forces are:

$|\vec{L}_{t/w}| = \frac{1}{2}\rho S_w\, {}^N\vec{v}^{Awing/tailAc}.\, {}^N\vec{v}^{Awing/tailAc} C_{L_{wing/tail}}$

$|\vec{D}_{t/w}| = \frac{1}{2}\rho S_t\, {}^N\vec{v}^{Awing/tailAc}.\, {}^N\vec{v}^{Awing/tailAc} C_{D_{wing/tail}}$

Taking moments about Acm,

$\sum \vec{M}^{A/Acm} = I_{yy}.{}^N\vec{\alpha}^{Acm}$

$\sum \vec{M}^{A/Acm} = I_{yy}\,\ddot{q}\vec{n}_y$ - (2)

From (1) and (2), there are 3 equations to solve for 3 unknowns $\ddot{q}, \ddot{x}, \ddot{z}$.

Solve

Case1:

Constants: Take-Off Speed (TOS) = 10 m/s, $q_o = 0°$, $\dot{q}_o = 0\ °/s$, a_t = -7.76°

Variable: Take-Off Angle (TOA)

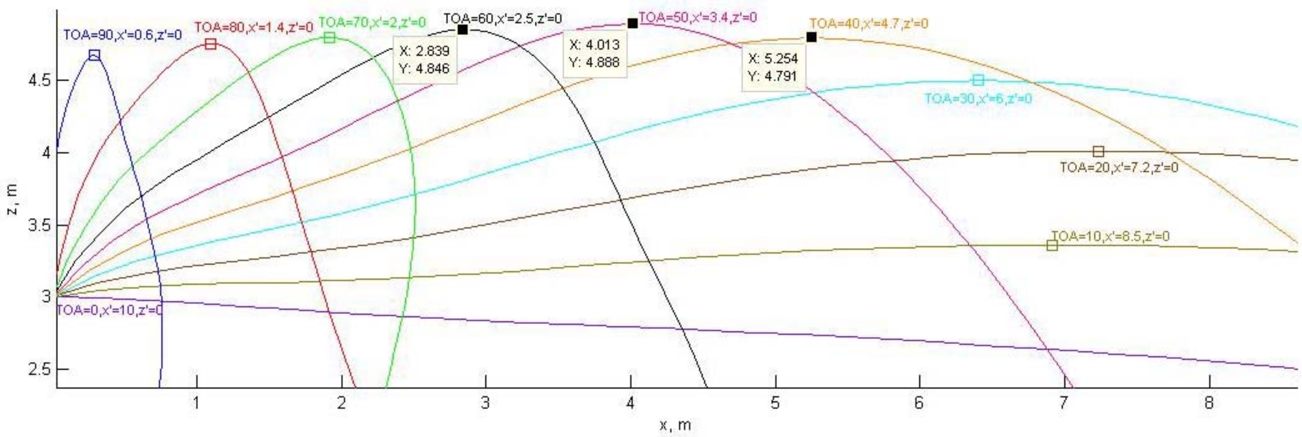

Figure(1). Jump trajectories for TOA: 0 °, 10 °, 20°, 30°, 40°, 50°, 60°, 70°, 80° and 90°

Case2:

Constants: Take-Off Angle (TOA) =$50°$,$q_o = 0°$, $\dot{q}_o = 0\ °/s$, a_t = -7.76°

Variable: Take-Off Speed

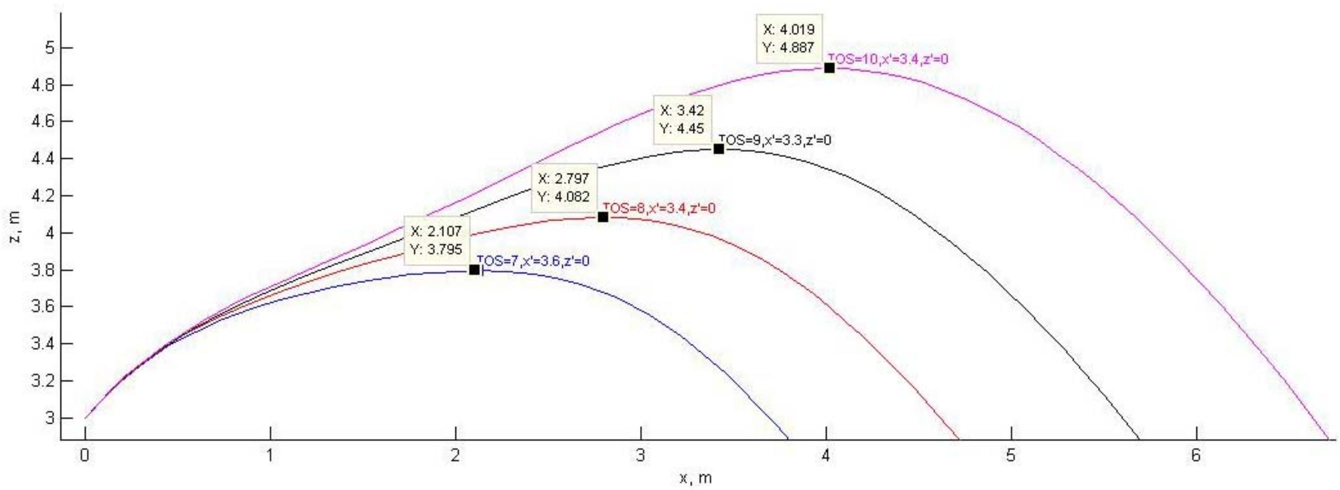

Figure(2). Jump trajectories for TOS: 7m/s, 8m/s, 9m/s, 10m/s

Interpretation

From figure(1), a TOA of 40° to 60° results in 3 of the highest jump heights. Any other TOA is not beneficial for obstacle clearance. The tradeoff is that the nx> measure of ${}^{N}\vec{v}^{Acm}$ decreases with increasing TOA. At $q_{initial} = 0°$, jumping at TOA>60° , the glider experiences the most energy loss due to drag. Therefore, TOA > 60° is not beneficial because the maximum jump height decreases and the nx> measure of ${}^{N}\vec{v}^{Acm}$ at its apogee are the lowest. For a fixed TOS of 10m/s, a potential choice of TOA is 50°.

Using a fixed TOA of 50°, the TOS on flight trajectory is examined. From figure(2), the TOS affects the glider's maximum jump height while the nx> measure of ${}^{N}\vec{v}^{Acm}$ at its apogee does not vary significantly with TOS

Design of launcher

What is the launcher's purpose?

To validate the simulation results, a launcher was designed to launch a mass of 0.5kg at a maximum speed of 10 m/s. The launcher consists of a pneumatic cylinder on a launch bed housed in a chamber that supports the launch table. The TOA can be adjusted from 20° to 90°. A launch bed can be angled via the holes on the side of the launcher. The TOS can be adjusted by varying the stroke length of the pneumatic cylinder.

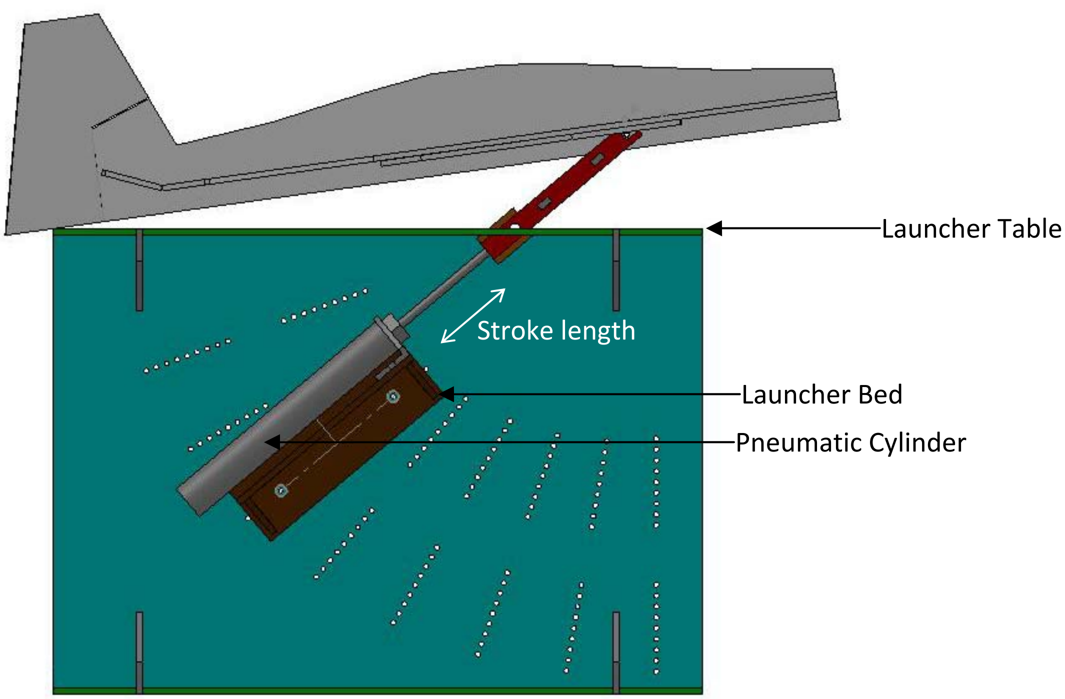

2. Analysis of EPFL 7g robot

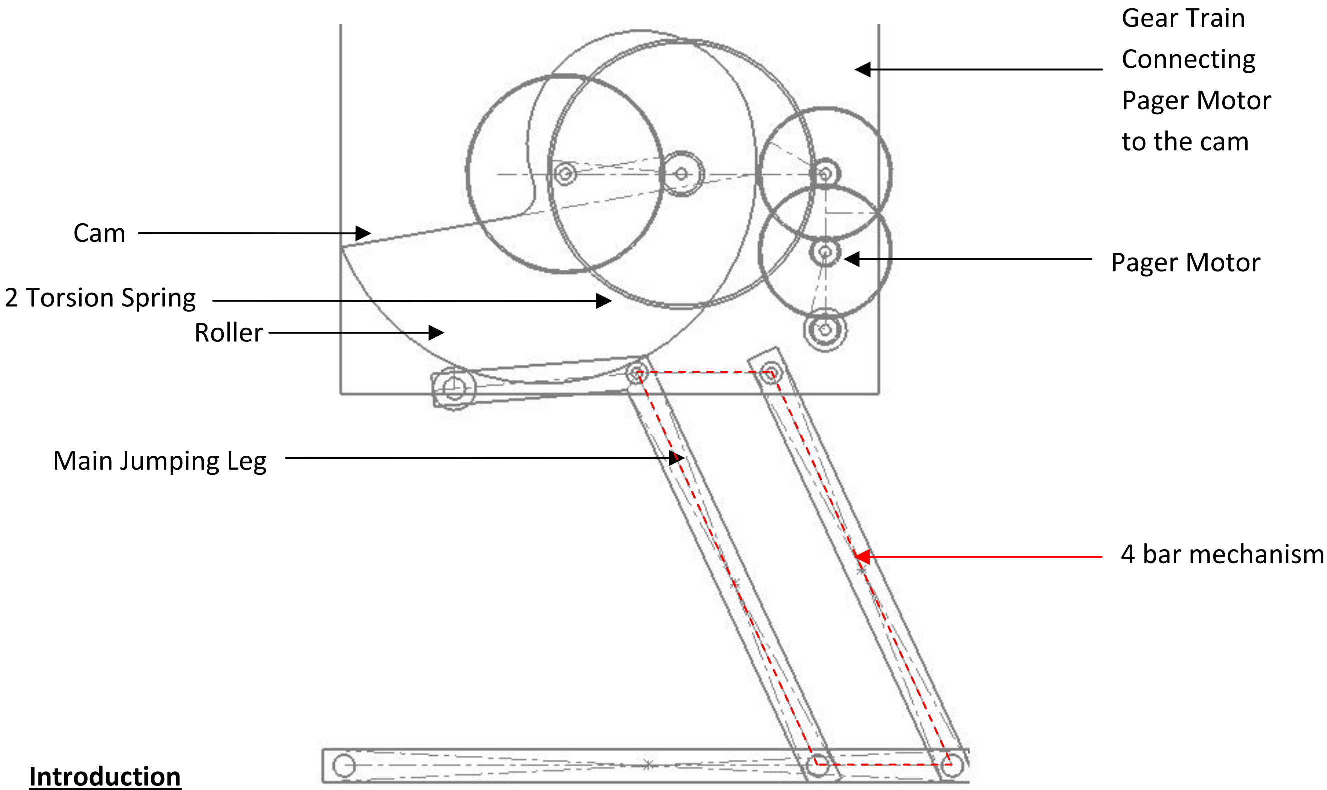

<u>Introduction</u>

My search for light jumping mechanisms to propel micro Unmanned Air-Vehicles (MUAV) into the air led me to study the EPFL 7g jumping robot. There are 3 questions to be addressed at the end of this analysis:

1. What is time history of the torque on the cam needed to drive it at a constant angular speed of 0.661 rad/sec? This would allow me to size the pager motor.
2. What is my take-off speed and take-off angle?
3. How does my simulation compare with actual results?

Modeling assumptions

- Simplified Model

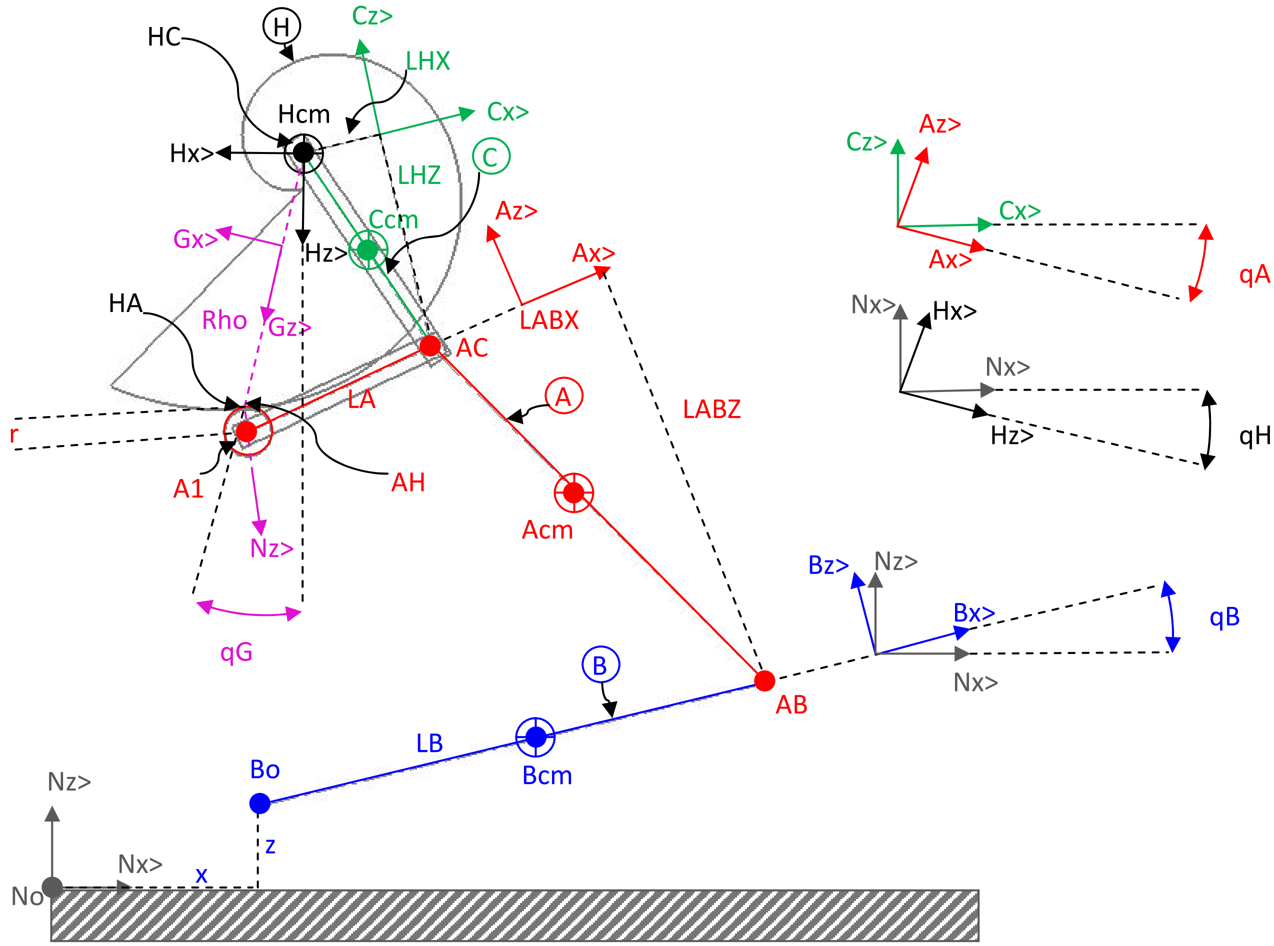

1. All links are rigid.
2. The contact between HA and AH is frictionless
3. To simplify the 4 bar mechanism, let C be fixed relative to B, ie qBC the angle between Cx> and Bx> is 0
4. The gear transmission and pager motor is replaced by an infinitesimally small motor at HC that applies a torque, $T^{H/C}$>, on H from C
5. The original 2 torsion springs are modeled as a single torsion spring at AC that applies a torque, $T^{A/C}$>, on A from C
6. Air resistance is negligible
7. Assume that no slipping occurs between both Bo and AB with the ground
8. No torsion damping is present

How does the mechanism work?

The motor drives the cam which charges the torsion spring. The cam continues charging the spring until the roller reaches the tip of the cam. As the motor continues to drive the cam, the energy stored in the spring is released when the roller passes the tip. This causes the jump of the mechanism.

Table of identifiers

Quantity	**Identifier**	**Type**	**(Initial) Value(s)**
parameter that defines shape of cam	a1	Constant	3 mm
local gravitational constant	g	Constant	9.80665 m/sec^2
Gear transmission ratio from pager motor to cam	GTR	Constant	1266
A's moment of inertia about Acm for Ay>	IAyy	Constant	223.6 g*mm^2
B's moment of inertia about Bcm for By>	IByy	Constant	73.1 g*mm^2
C's moment of inertia about Acm for Cy>	ICyy	Constant	350 g*mm^2
H's moment of inertia about Hcm for Hy>	IHyy	Constant	54.4 g*mm^2
Torsional spring constant	k	Constant	0.0836 N*m/rad
Distance of A1 from AC	LA	Constant	17 mm
Ax> measure of AB from AC	LABX	Constant	13.7 mm
Az> measure of AB from AC	LABZ	Constant	37.6 mm
Distance of AB from Bo	LB	Constant	44 mm
Cx> measure of HC from AC	LHX	Constant	-6.65 mm
Cz> measure of HC from AC	LHZ	Constant	18.4 mm
Mass of A	mA	Constant	0.76 g
Mass of B	mB	Constant	0.453 g
Mass of C	mC	Constant	5.253 g
Mass of H	mH	Constant	0.78 g
Angle between Cz> and Bz>	qBC	Constant	0 rad
Natural angle of the torsional spring	qN	Constant	π rad
radius of the roller on A	r	Constant	2 mm
desired operating angular velocity of cam	wH	Constant	-0.661 rad/sec
qA is defined as the angle between Cx> and Ax> in the positive Ay> direction	qA	dependent variable	
qB is defined as the angle between Nx> and Bx> in the negative By> direction	qB	dependent variable	
qG is a geometric angle that orients the point of contact of H on A	qG	dependent variable	
qH is defined as the angle between Nz> and Hz> in the positive Hy> direction	qH	independent variable	(π rad)
Work of forces on the system	work	dependent variable	(0 joules)
Nx> measure of Bo from No	x	dependent variable	(0 mm)
Nz> measure of Bo from No	z	dependent variable	(0 mm)
Fn is the normal force acting on HA from AH	Fn	dependent variable	
RBoX is the Nx> measure of the force on Bo	RBoX	dependent variable	
RBoZ is the Nz> measure of the force on Bo	RBoZ	dependent variable	
RABZ is the Nz> measure of the force on AB	RABZ	dependent variable	
Operating torque of motor	Tm	dependent variable	
Surface function of the cam measured from HC to point of contact with A	rho	specified	

Physics

The simulation is broken into 4 states:

1. Charging the torsion spring at an angular speed 0f -0.661 rad/sec
2. Roller passes the tip of the cam when qG>6.9 rad
    a. At qG = 6.9 rad, the tip of the cam is reached.
    b. Check if the normal force acting on AB is positive.
        i. If positive remain in state 2 else exit state 2
3. In State 3 the constraint holding AB to the ground is broken.
    a. Check if the normal force acting on Bo is positive
        i. If positive remain in state 3 else exit state 3
4. In State 4, the mechanism is free from configuration constraints. Jump has occurred

At each state, Kane's method is used to derive the Equations Of Motion (EOM). MG was used to derive the equations at each state. Then, the EOM of each state was combined in MATLAB to perform a full simulation of the jump sequence.

Enter when:	qG<6.9 rad		Enter when:	RABZ>0		Enter when:	RBoZ>0		Enter when:	RBoZ<0	
Exit when:	qG>6.9 rad		Exit when:	RABZ<0		Exit when:	RBoZ<0		Exit when:	simulation time stops	
STATE 1		→	**STATE 2**		→	**STATE 3**		→	**STATE 4**		
MotionVariable'	Variable	Specfied	MotionVariable'	Variable	Specfied	MotionVariable'	Variable	Specfied	MotionVariabl e'	Variable	Specfied
qH''	qG''		qA''	RBoX	qH' ;=0	qA''	RBoX	qH' ;=0	qA''		qH' ;=0
qA''	Fn		qB''	RBoZ	qG' ;=0	qB''	RBoZ	qG' ;=0	qB''		qG' ;=0
qB''	Tm		X''	RABZ	Fn = 0	X''		Fn = 0	X''		Fn = 0
X''	RBoX		z''		Tm = 0	z''		Tm = 0	z''		Tm = 0
z''	RBoZ							RABZ=0			RABZ=0
	RABZ										RBoX=0
11unkowns			7 unkowns			6 unkowns			4 unkowns		RBoZ=0
5 kane equations	5 configuration constraints		4 kane equations	3 configuration constraints		4 kane equations	2 configuration constraints		4 kane equations		
	qH' ;=-0.661 rad/sec										
11equations			7 equations			6 equations			4 equations		

Solve

- Results

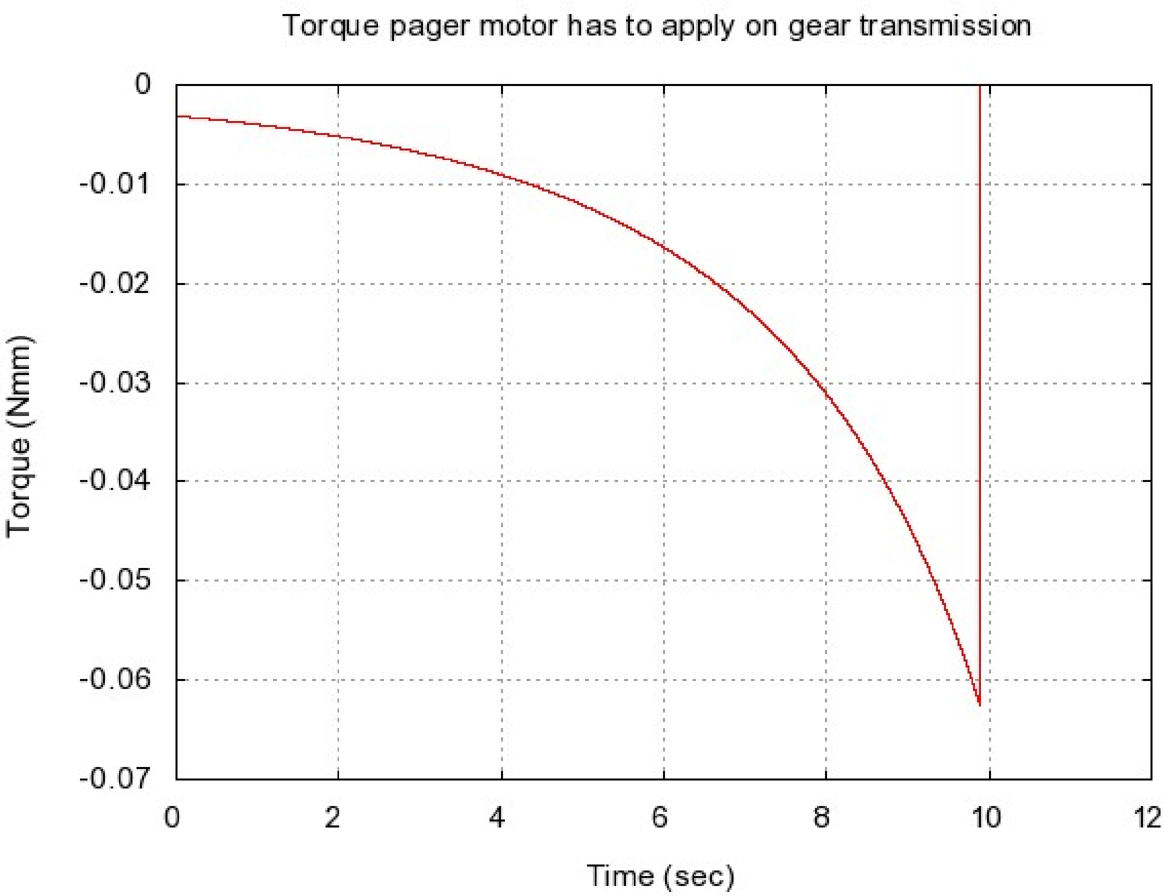

Figure (3). From State 1, the pager motor torque, Tm, required to actuate the cam at a constant angular velocity of -0.661 Ny> is backed out of the EOM

According to the paper written on the EPFL jumper, their cam was designed so that the pager motor applies a constant torque of -0.038Nmm to drive the cam at a constant angular velocity of -0.661 Ny>. This could have been done to ensure the pager motor is operating in its most efficient torque setting. In this analysis, I picked a spiral using the golden ratio as a function to describe my cam surface. This shape is not designed to load the pager motor optimally. As seen in figure(3), the required torque increases to a maximum of approximately -0.06 Nmm. Knowing this, I can size my pager motor based on a required torque of 0.06 Nmm.

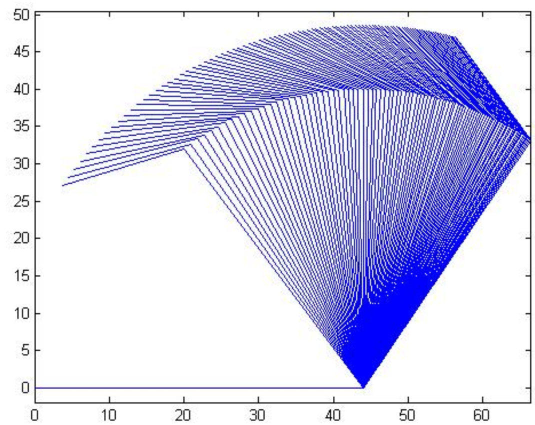

Figure (4.1). State 1: cam charging spring

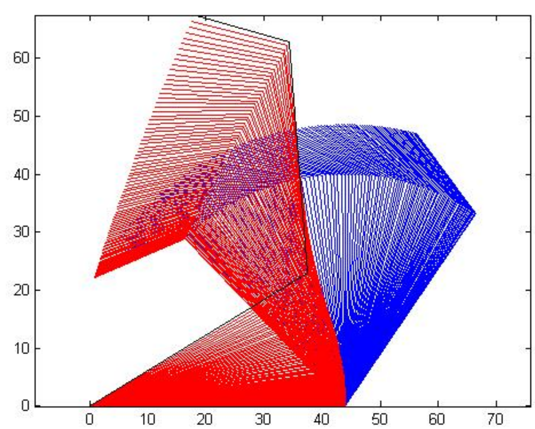

Figure (4.2). State 3: RABZ<0, point AB is no longer constrained to the ground

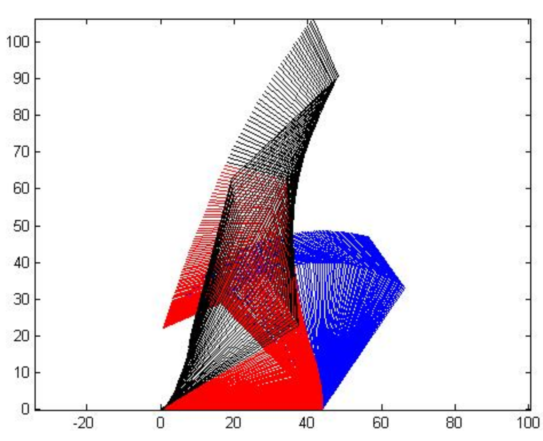

Figure (4.3). State 4: RBoZ<0, point Bo is no longer constrained to the ground. Jumper has taken off .

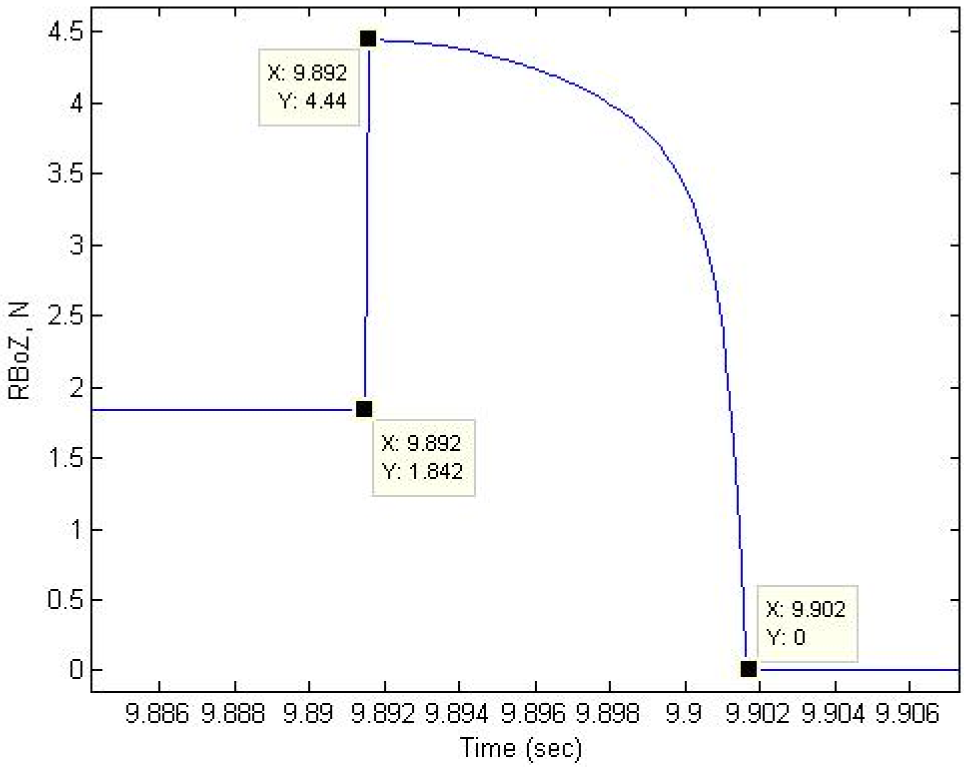

Figure (5). From the force history of RBoZ, transitions from state 1 to State 3 is observed at t=9.892 sec. The peak force on Bo is 4.44N. Take off is observed at t=9.902 sec

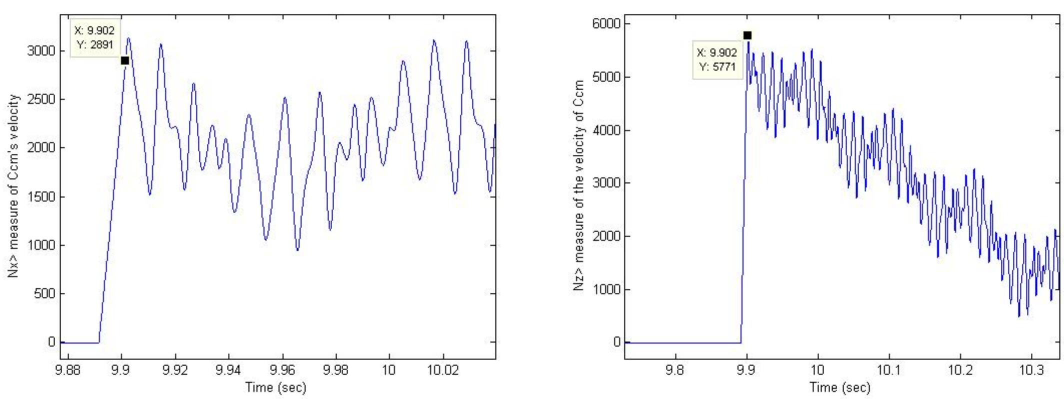

Figure (6). At t=9.902, the jumper has taken off. The Nx> measure of Ccm's velocity is 2891 mm/sec. The Nz> measure of Ccm's velocity is 5771 mm/sec

Based on results from figure(5)&(6), the take of speed is:

Take-off speed = $(2.891^2+5.771^2)^{0.5}$ = 6.45 m/sec

Take-off angle = atan(5.771/2.891) = 63 deg

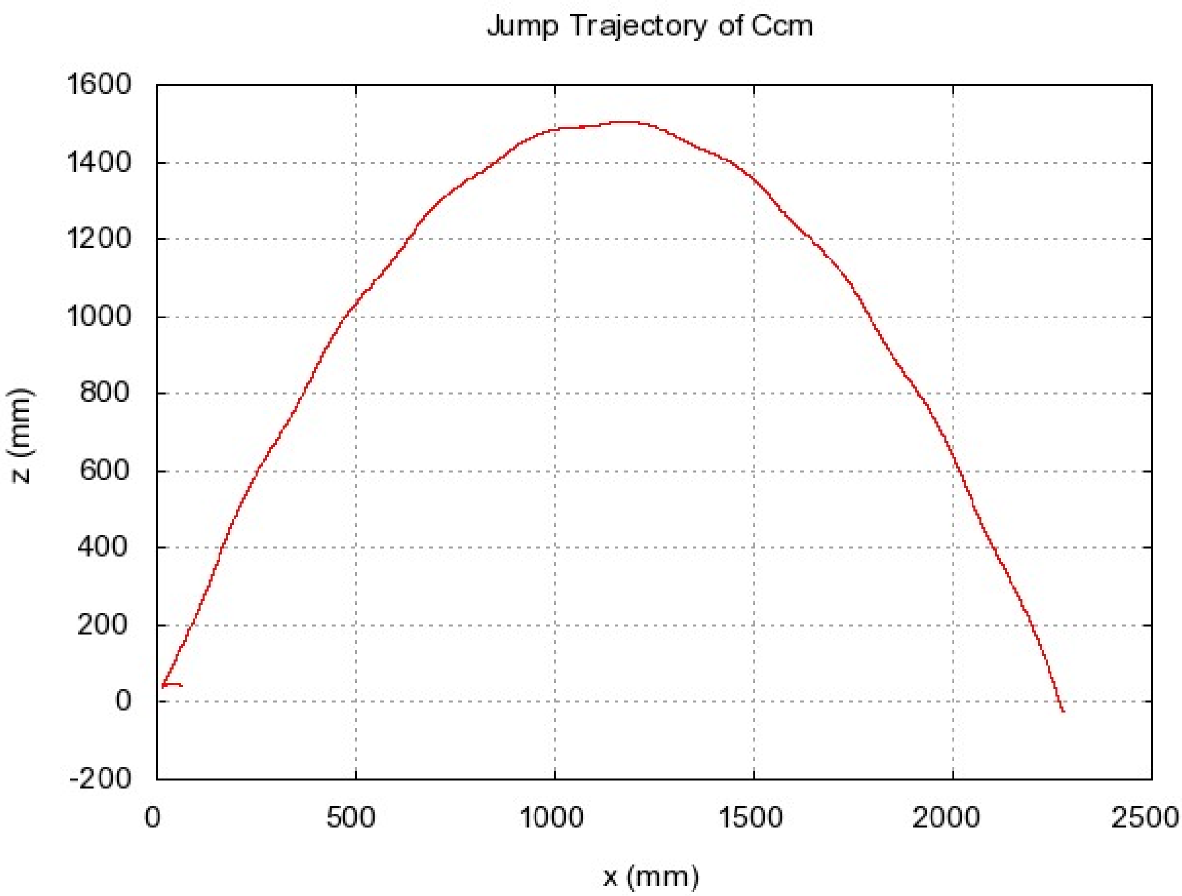

Figure (7). Max height achieved was approximately 1.5m

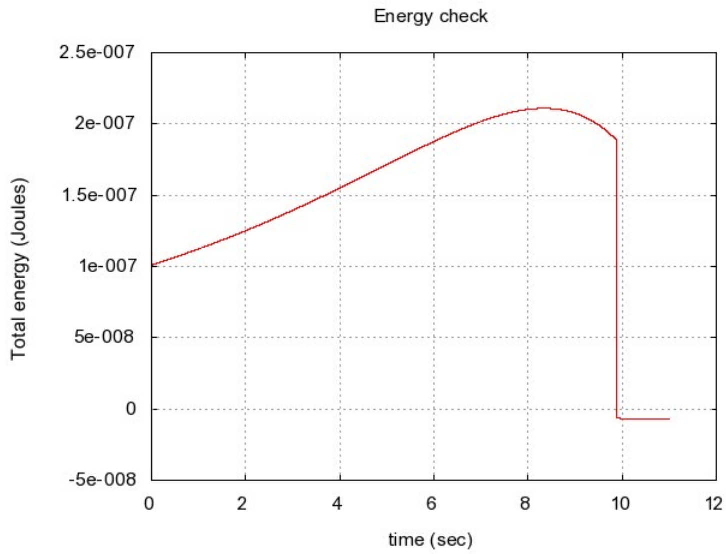

Figure (7). The total energy in the system remains at 0.

Interpretation

How does the simulation compare to actual experimental data?

	experiment	simulation
Take off speed (m/sec)	5.9	6.45
Take off angle (deg)	75	63
max height (m)	1.4	1.5

The simulation compares favorably to the experiments. The discrepancies are due to assumptions made as well modeling simplifications. The increase in max height for the simulation is most likely due to the absence of air resistance in state 4.

This simulation has enabled me to understand how the EPFL jumper performs its jumps. It has also provided me with a tool to design jump mechanisms by allowing me to:

1. Design cams for various motors by looking at the torque history
2. Design jump trajectories by changing leg lengths and torsion spring constants.

Summary and future work

The first section focused on building a simulator to simulate a jumping glider. Then, a launcher was built to validate simulation results.

From simulation, a potential TOA is 50°. The effect of TOS is less obvious. Therefore, I hope to use the physical launcher to ascertain the appropriate TOS.

The second section focused on the analysis of the EPFL jumper. The reason I pursued such an analysis was to start looking at different ways of integrating a jumping mechanism with a small UAV.

There are similarities between perching and jumping. The perching mechanism prevents the UAV from falling off the wall while the jumping mechanism propels the UAV into the air by gripping the jump surface to prevent slippage. Ideally, the mechanism that allows the UAV to perch should also be able to act as a jumping mechanism for take-off.

Another question that should be addressed is the energy benefit/penalty jumping poses.